

Range of validity of the Rayleigh hypothesis

T. Watanabe,¹ Y. Choyal,² K. Minami,² and V. L. Granatstein³

¹*Theory and Data Analysis Division, National Institute for Fusion Science, Toki City 509-5292, Japan*

²*Graduate School of Science and Technology, Niigata University, Niigata City 950-2181, Japan*

³*Institute for Research in Electronics and Applied Physics, University of Maryland, College Park, Maryland 20742, USA*

(Received 5 October 2003; published 14 May 2004)

The parameter range over which the Rayleigh hypothesis (RH) for optical gratings might be validly applied to analysis of high power backward wave oscillators has been investigated numerically. It had been pointed out that from a rigorous mathematical viewpoint, RH was only valid for a shallow corrugation of slow wave structure (SWS) such that $hK_0 < 0.448$; here, h and K_0 are, respectively, the amplitude and wave number of the periodicity in a sinusoidal planar grating. We numerically analyze the electromagnetic fields in the axisymmetric SWS with and without use of RH. The field patterns and eigenfrequency for the SWS are solved numerically for a given k_z by using the code HIDM (higher order implicit difference method) that is free from the RH. It is found that, for a deep corrugation, $hK_0 = 5 \times 0.448$, using RH is still valid for obtaining the dispersion relation, although the Floquet harmonic expansion (FHE) fails to correctly represent the field patterns inside the corrugation. Accordingly, there exists a discrepancy between the validity of using RH for obtaining dispersion relations and for an exact convergence of FHE everywhere in the SWS.

DOI: 10.1103/PhysRevE.69.056606

PACS number(s): 42.25.Fx, 02.60.Lj, 02.70.Bf, 84.40.Fe

A widely used method for analyzing high power backward wave oscillators (BWO's) is to represent the electromagnetic (EM) fields in the axisymmetric slow wave structure (SWS) in terms of a Floquet harmonic expansion (FHE). In this expansion, the EM fields, \mathbf{E} and \mathbf{B} , with angular frequency ω and wave number k_z in axial direction are expressed in the form,

$$\begin{bmatrix} \mathbf{E} \\ \mathbf{B} \end{bmatrix} = \sum_{n=-N}^N \begin{bmatrix} \mathbf{E}_n(r) \\ \mathbf{B}_n(r) \end{bmatrix} \exp i(k_{zn}z + l\theta - \omega t), \quad (1)$$

where $k_{zn} = k_z + nK_0$, K_0 is the wave number of the SWS periodicity, and $n=0, \pm 1, \pm 2, \dots, \pm N$ is the Floquet harmonic number. The value of N , in principle, is infinite. Expansion similar to Eq. (1) was first introduced by Lord Rayleigh for diffraction of waves from planar gratings [1]. He assumed that the expansion was applicable both outside and inside the corrugation, and this assumption is known as the Rayleigh hypothesis (RH). Recently, some mathematicians objected to our application of Eq. (1) to a particular BWO analysis [2]. It was argued that our numerical analysis was applied to a deep corrugation of $hK_0 = 1.67$ which is 3.7 times the limiting value for validity in the RH for a planar sinusoidal grating, consequently the results were deemed invalid. Here, h is the amplitude of sinusoidal corrugations in the SWS. It was somewhat surprising, however, that our analytical results seemed to be valid even in the case $hK_0 = 1.67$, where many BWO experiments and analyses have been carried out [3]. The paradoxical discrepancy in the validity between conventional analyses of high power BWO's and mathematical requirement for RH in planar gratings must be investigated in further details. To respond to this necessity, EM fields and dispersion relation in the SWS are numerically analyzed with and without RH for a given set of size parameters in the present paper.

Doubts concerning the validity of the RH were aroused as early as the 1950s by Deriugin [4] and Lippmann [5] in the course of analyzing the problem of diffraction of plane waves by a periodic grating. The limiting conditions of the RH for sinusoidal planar gratings were investigated by Petit [6] and Millar [7]. Yasuura and his collaborators developed an improved point-matching method for calculating correctly finite terms of FHE for deeper corrugations than $hK_0 = 0.448$ of sinusoidal planar grating [8,9]. The fundamental problem involves the location of singularities in the complex representation of the given profile of the gratings. Berg and Fokkema have elegantly discussed the method of obtaining this singularity for various geometries [10,11]. The limit of validity of Eq. (1) for sinusoidal planar grating is obtained as $hK_0 < 0.448$ from the condition that the circle of convergence touches critically the singularity arising from the curve of the corrugation. The condition $hK_0 < 0.448$ is not a universal condition for RH, but it is applicable only for sinusoidal planar gratings. Mathematical reports dealing with the validity of the RH for empty periodic axisymmetric SWS used in BWO's have not appeared up to date. We numerically investigate the convergence of Eq. (1) for an axisymmetric SWS with a chosen set of size parameters. We show that a valid dispersion relation is obtained even at $hK_0 = 5 \times 0.448$, which is much greater than the limiting value 0.448 of the RH for the planar sinusoidal gratings.

Hereafter, we limit ourselves to the analysis of EM fields with and without using Eq. (1) in sufficiently long metal axisymmetric SWS without electron beam in which the inner wall radius is given by,

$$R(z) = R_0 + h \cos K_0 z, \quad K_0 = 2\pi/L, \quad (2)$$

where L is the length of periodicity. In the planar gratings quoted above, the diffracted waves outside do not enter again into the gratings, so what one has to solve is just a boundary

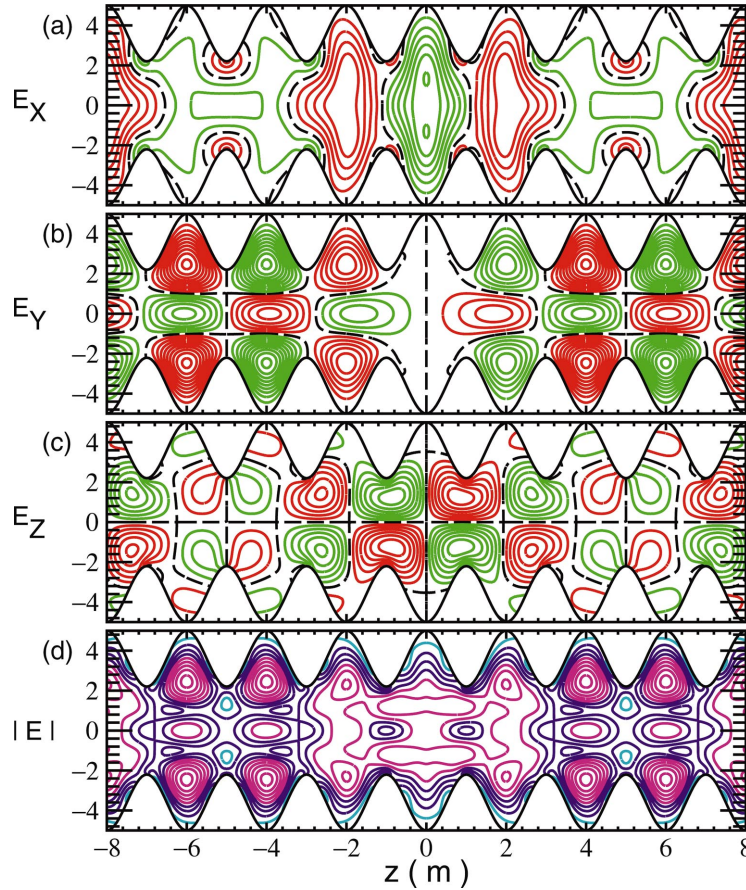


FIG. 1. (Color) Electromagnetic field patterns of the quasi- TE_{13} mode calculated by difference code scheme HIDM (higher order implicit difference method) that is free from the Rayleigh hypothesis. Given numerical parameters are shown in the text. In (a) E_x , (b) E_y , (c) E_z and (d) $|\mathbf{E}|$ are, respectively, normalized by the maximum value in one period in the axial direction. The red and green curves in (a)–(c) are, respectively, positive and negative contours of the normalized field components, each adjacent curves showing difference in value of 0.1. Contour of normalized values of $|\mathbf{E}|=\text{constant}$ are depicted in (d). Sky blue, blue, and pink curves are, respectively, for $|\mathbf{E}|\leq 1/6$, $1/6 < |\mathbf{E}|\leq 1/2$, and $1/2 < |\mathbf{E}|\leq 1$.

value problem. In other words, frequency ω and k_z of an incident plane wave can be chosen independently. In the present SWS, however, diffracted wave becomes incident wave again, so, ω and wave number k_z are combined by a dispersion relation. In other words, it is an eigenvalue problem in addition to a boundary value problem. First, the field patterns and eigenfrequency for the SWS are solved for a given k_z numerically by using the code HIDM (higher order implicit difference method) that is free from the RH. The HIDM has been constructed to solve numerically in general algebraic equations, ordinary and partial differential equations and their coupled equations with high numerical accuracy and high numerical stability [12]. Discretization error of the HIDM is, in the present analysis, $O(\Delta x^9)$ much higher than conventional schemes of the Runge-Kutta method that usually has errors $O(\Delta x^4)$ or $O(\Delta x^6)$. Here, Δx is the element of difference scheme. An example of EM fields for a quasi- TE_{13} mode in the SWS solved by the HIDM is shown in Fig. 1. Maxwell's equations are solved numerically in cylindrical coordinates with difference scheme in the axial direction and the HIDM in the radial direction. Here, $R_0 = 3.6$ m, $h = 1.4$ m, and $L = 4.0$ m are chosen in Eq. (2). The wave number is $k_z = 0.4K_0$ that corresponds to a wave-

length of 10 m. The frequency of the EM fields is obtained to be the eigenvalue of 79.12 MHz for the assumed value of k_z . The EM fields are at the instant $t = 0.75T$, where T is the period of oscillation. Cartesian components of electric field, (a) E_x , (b) E_y , and (c) E_z are normalized by the maximum value of $|\mathbf{E}|$ in a period. The periodic length L is divided into equal 36 segments and equal 72 segments in radial direction from the axis to $R(z)$ given by Eq. (2). On each grid point, the Cartesian components of electric field are calculated. The red and green curves are, respectively, positive and negative contours of the normalized field components, adjacent curves showing difference in value of 0.1. Dashed black lines show zero value lines that divide red and green contours. Contour of $|\mathbf{E}|=\text{constant}$ is depicted in (d). The values are again normalized by the maximum value of $|\mathbf{E}|$ in a period. Sky blue, blue and pink curves are, respectively, $|\mathbf{E}|\leq 1/6$, $1/6 < |\mathbf{E}|\leq 1/2$, and $1/2 < |\mathbf{E}|\leq 1$. Electric fields are concentrated in the pink regions. It is confirmed that electric field lines are perpendicular to the metal surface given by Eq. (2). It was determined that the HIDM can calculate various EM modes in the SWS accurately and without accumulation of numerical errors.

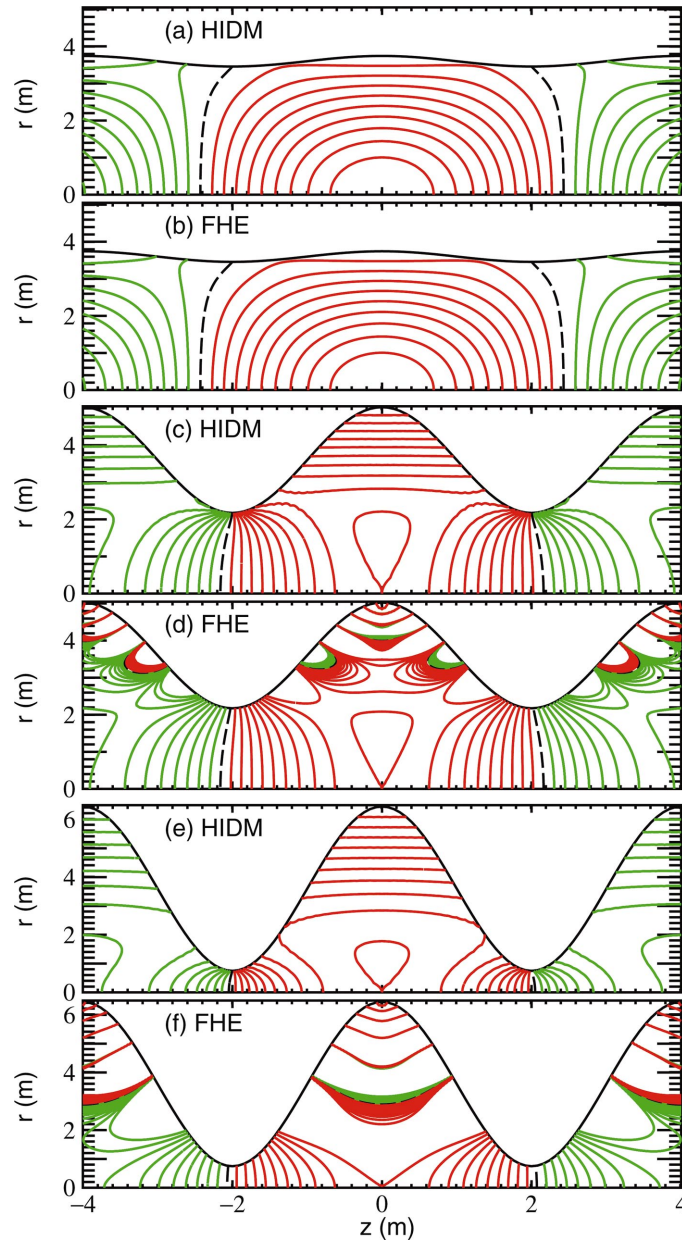


FIG. 2. (Color) Comparison of the normalized field component E_z with and without Rayleigh hypothesis (RH). Size parameters but h are $R_0=3.6$ m and $L=4.0$ m in Eq. (2). (a), (c), and (e) are obtained by the HIDM that is free from the RH, and (b), (d), and (f) are from the RH. Normalization is to the value of E_z at $z=0$ and $r=0$. Each contour shows a difference of 0.1 to its adjacent curve. (a) and (b) are a shallow corrugation case of $hK_0=0.5 \times 0.448$, and both results are exactly identical. (c) and (d) are a relatively deep corrugation case of $hK_0=5 \times 0.448$, and both results are identical near the axis, but quite different inside the corrugation. (e) and (f) are an extremely deep corrugation case of $hK_0=10 \times 0.448$, and both results are different everywhere in the slow wave structure.

Secondly, we solve numerically the field patterns and eigenfrequency for the SWS as shown in Fig. 1 for a given wave number k_z by using FHE Eq. (1). Our method of numerical calculation by FHE is as was shown in Ref. [3] without electron beam. In FHE, the number of terms to calculate is denoted by N that is the maximum value of $|n|$ in Eq. (1). Then, coupled simultaneous linear equations including $2N+1$ unknown coefficients of EM fields in Eq. (1) are obtained from the boundary condition that the tangential components of RF electric field at the metal surface must be zero. The dispersion relation between ω and k_z is given by the require-

ment that the $(2N+1) \times (2N+1)$ determinant must be zero. Once the relation is determined, one can calculate the relative magnitudes between the $2N+1$ coefficients that enable us to analyze field patterns numerically. The results for TM_{01} mode E_z =constant contours, calculated by HIDM and by FHE are compared with each other in Fig. 2 for $k_z=0.4K_0$ and for three values of $hK_0=0.5 \times 0.448$, 5×0.448 , and 10×0.448 . We have chosen here to be $N=6$ in Eq. (1). In Fig. 2, the values of field are normalized by the value of E_z at $z=0$ and $r=0$. Each contour shows a difference of 0.1 to its adjacent curve. In Figs. 2(a) and 2(b), the results of HIDM

and FHE are shown, respectively, for a case of shallow corrugation $hK_0=0.5 \times 0.448$. Both results (a) and (b) are identical, and no distinction between them is possible. This fact means that FHE is exactly valid in this case. The results for a somewhat deep corrugation $hK_0=5 \times 0.448$ are compared in Fig. 2(c) HIDM and (d) FHE. Inside the corrugation, the field patterns are quite different from each other. In (d) with FHE, very large values of nonphysical undulating E_z inside the corrugation are caused by the presence of terms with modified Bessel functions in Eq. (1). Whereas, in (c) with HIDM, no such nonphysical fields are found. In order that Eq. (1) satisfies the boundary condition at the metal surface exactly, extremely large values of field components are observed between red or green crescent moons at the trough of corrugation as shown in (d). If the number of digits in numerical computation and N in Eq. (1) are infinitely large, such nonphysical large undulations are expected to disappear. The number of undulations at the bottom of corrugation is given by N in Eq. (1). It is noted, however, that the field patterns outside the corrugation, where beam microwave interaction takes place, coincide quite well with each other in (c) and (d), even for such a deep corrugation. The results for an exceedingly deep corrugation $hK_0=10 \times 0.448$ are shown in Fig. 2 (e) HIDM and (f) FHE, respectively. The E_z 's are different from each other not only inside the corrugation but also outside near the center axis. This fact suggests that FHE is completely violated for this case of deep corrugation.

The results of the dispersion relation for TM_{01} mode calculated by both HIDM and FHE are compared for three values of $hK_0=0.5 \times 0.448$, 5×0.448 and 10×0.448 in Fig. 3. We have chosen again to be $N=6$ in FHE Eq. (1). In Fig. 3(a), the results of HIDM (black circles) and FHE (continuous curve) are shown, respectively, for the case of shallow corrugation $hK_0=0.5 \times 0.448$. Both results are identical, and no distinction between them is possible. This means that FHE is exactly valid in this shallow case. The curve has an exact periodicity of $K_0=1.571 \text{ m}^{-1}$ with respect to wave number k_z that is required by Floquet theorem for any periodic structure. The results for a deep corrugation $hK_0=5 \times 0.448$ are shown in Fig. 3(b) by black circles (HIDM) and a curve (FHE). Both results agree well with each other, and have again correctly a periodicity of $K_0=1.571 \text{ m}^{-1}$ with respect to the wave number k_z that is required by Floquet theorem. The FHE is still valid even though Eq. (1) is locally nonconvergent as is shown in Figs. 2(c) and 2(d) inside the corrugation. The results for an exceedingly deep corrugation $hK_0=10 \times 0.448$ are shown in Fig. 3(c) FHE with $N=4$ in Eq. (1), (d) FHE with $N=6$ in Eq. (1) and (e) HIDM. In (c) and (d), the curves no longer satisfy periodicity for the wave number k_z between 0 and $K_0=1.571 \text{ m}^{-1}$ that is required by the Floquet theorem. This fact suggests that FHE becomes invalid in the deep corrugation $hK_0=10 \times 0.448$ for obtaining the dispersion relation. On the other hand, in (e) HIDM, the dispersion curve satisfies Floquet periodicity exactly.

The dependence on the number N of the terms to calculate correctly FHE in Eq. (1) is investigated in Fig. 4. Here, eigenfrequencies $\omega/2\pi$ at wave number $k_z=0$ are calculated for various values of N in horizontal axis. In case $hK_0=0.5 \times 0.448$, shown by black circles, $N=2$ in Eq. (1) is sufficient to obtain $\omega/2\pi=30.9 \text{ MHz}$ for $k_z=0$ as shown in Fig. 3(a).

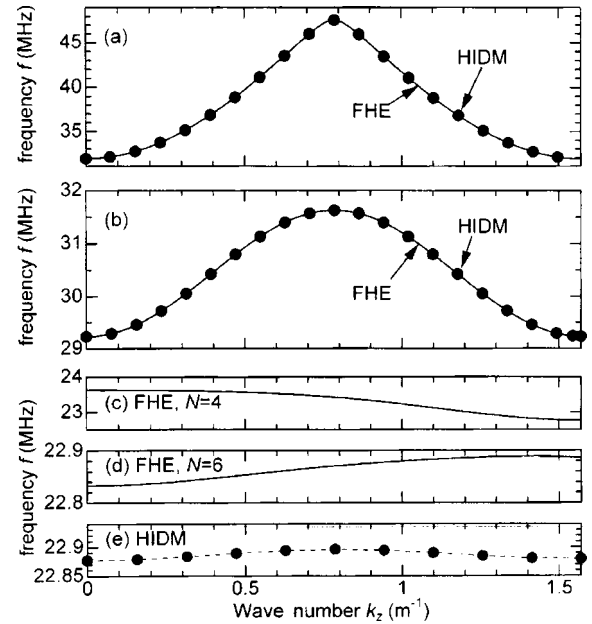


FIG. 3. Comparison of dispersion relation for TM_{01} mode with and without the RH. Size parameters but h are the same as those in Fig. 2. (a) A case of shallow corrugation $hK_0=0.5 \times 0.448$, and (b) a case of deep corrugation $hK_0=5 \times 0.448$. In both (a) and (b), continuous curves and black circles are, respectively, with and without the RH. Both results coincide sufficiently well, even though in case of (b) the field patterns are locally incorrect as is shown in Fig. 2(d) given by the RH. (c), (d), and (e) are the case of exceedingly deep corrugation $hK_0=10 \times 0.448$. (c) and (d) are from the RH, and the results do not satisfy the Floquet periodicity theorem. (e) Black circles combined with dashed curves are from HIDM, and the results satisfy the Floquet periodicity theorem exactly.

In case $hK_0=5 \times 0.448$, shown by white squares, $N=5$ is required to obtain $\omega/2\pi=29.2 \text{ MHz}$ for $k_z=0$ as shown in Fig. 3(b). In case $hK_0=10 \times 0.448$, shown by black triangles, $N=5$ is still insufficient to obtain $\omega/2\pi=22.88 \text{ MHz}$ for $k_z=0$ as shown in Fig. 3(e) calculated by HIDM. In conclusion, the value of N must be increased with increase in hK_0 , even if the FHE is applicable.

The FHE in Eq. (1) can be a complete set of functions only for any waves in free space or in rectangular cubes. The

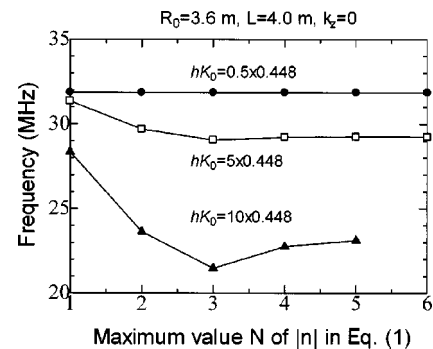


FIG. 4. The dependence on the number N of the terms required to calculate correctly FHE in Eq. (1). Here, eigenfrequencies $\omega/2\pi$ at wave number $k_z=0$ are calculated for various values of N in horizontal axis. Size parameters but h are the same as those in Fig. 2. The value of N must be increased with an increase in hK_0 .

FHE is an incomplete set of functions to express waves in the SWS we are considering or in other gratings. For this reason, it is not strange that the FHE given in Eq. (1) breaks down to express waves in a case of deep corrugation.

Coincidence of the dispersion relation obtained from Eq. (1) and that from HIDM up to $hK_0=5 \times 0.448$ leads us to assert that the FHE using the RH is valid and works well for the parameters of SWS beyond the limitation $hK_0 < 0.448$. The statement that FHE is valid up to 5 times the limit $hK_0=0.448$ in planar grating was made previously in Ref. [13]. For this range, a correct dispersion relation can be obtained, even though there is no convergence of FHE at every point in the SWS. In other words, the dispersion relation can be insensitive to a local breakdown of RH in cases of moderately deep corrugation. This result agrees with a general

fact that the eigenvalues converge faster than the fields in many eigenvalue problems. The analysis of BWO's using HIDM can reveal much about higher order modes that are found to creep along the corrugated surface, whereas such information is lost if FHE is used. However, the analysis of HIDM requires huge computation time and resources. Roughly speaking, one hundred times more computation time is necessary in using HIDM compared with using FHE. Equation (1) of the RH is a simple and convenient way to analyze the SWS in high power BWO's, if analysis is restricted to lower frequency modes. In the present paper, the practical range of validity of the RH in the analysis of axisymmetric SWS is shown for a chosen set of numerical parameters. It is important to clarify the limit of validity of the RH in a more generalized mathematical manner.

-
- [1] Lord Rayleigh, Proc. R. Soc. London, Ser. A **79**, 399 (1907).
 [2] K. Minami *et al.*, IEEE Trans. Plasma Sci. **30**, 1134 (2002).
 [3] See for example, J. A. Swegle *et al.*, Phys. Fluids **28**, 2882 (1985).
 [4] L. N. Deriugin, Dokl. Akad. Nauk SSSR **87**, 913 (1952).
 [5] B. A. Lippmann, J. Opt. Soc. Am. **43**, 408 (1953).
 [6] R. Petit Edited, *Electromagnetic Theory of Gratings* (Springer-Verlag, New York, 1980), p. 61.
 [7] R. F. Millar, Proc. Cambridge Philos. Soc. **65**, 773 (1969).
 [8] H. Ikuno and K. Yasuura, IEEE Trans. Antennas Propag. **21**, 657 (1973).
 [9] T. Matsuda and Y. Okuno, J. Opt. Soc. Am. A **7**, 1693 (1990).
 [10] P. M. van den Berg and J. T. Fokkema, J. Opt. Soc. Am. **69**, 27 (1979).
 [11] P. M. van den Berg and J. T. Fokkema, IEEE Trans. Antennas Propag. **27**, 577 (1979).
 [12] T. Watanabe, Ann. Numer. Math. **1**, 293 (1994).
 [13] E. G. Loewen and E. Popov, *Diffraction Gratings and Applications* (Marcel Dekker, New York, 1997), Chap. 10 p. 374.